COMMISSIONS G1 AND G4 OF THE IAU
INFORMATION BULLETIN ON VARIABLE STARS
Volume 62 Number 6192 DOI: 10.22444/IBVS.6192

Konkoly Observatory
Budapest
2 January 2017

HU ISSN 0374 – 0676

V2477 Cyg — A W–TYPE CONTACT ECLIPSING BINARY

NELSON, ROBERT H.[1,2]

[1] 393 Garvin Street, Prince George, BC, Canada, V2M 3Z1
email: bob.nelson@shaw.ca

[2] Guest investigator, Dominion Astrophysical Observatory, Herzberg Institute of Astrophysics, National Research Council of Canada

The variability of V2477 Cyg (NSV 13016 = NSVS 3227395 = HD 239379 = TYC 3945–1423–1), amongst many others, was discovered photographically by Hoffmeister (1963) as part of the Sonneberg Survey (Gessner 1966). The former gave coordinates and a finder chart, described the system as a short period variable, and designated it as S 7891. Skiff (1999) identified many Sonneberg variables, amongst them S 7891, giving accurate coordinates and associating them with existing names. The first accessible elements (epoch, period) were published by Otero & Wils (2005), who also classified the system as EW, and listed the magnitude range and spectral type. Since then, there have been a number of eclipse timings, but no light curve analysis.

In order to rectify this lack, the author first secured, in April of 2015 and again in September of 2016, a total of 6 medium resolution (R∼10000 on average) spectra of V2477 Cyg at the Dominion Astrophysical Observatory (DAO) in Victoria, British Columbia, Canada using the Cassegrain spectrograph attached to the 1.85 m Plaskett Telescope. He used the 21181 grating with 1800 lines/mm, blazed at 5000 Å giving a reciprocal linear dispersion of 10 Å/mm in the first order. The wavelength ranged from 5000 to 5260 Å, approximately. A log of observations is given in Table 1. The following elements were used for both radial velocity (RV) and photometric phasing:

$$JD(\mathrm{Hel})_{\mathrm{MinI}} = 2457176.2636 + 0.3112515\,\mathrm{E} \qquad (1)$$

Frame reduction was performed by software 'RaVeRe' (Nelson 2009). See Nelson et al. (2014) for further details. The normalized spectra are reproduced in Fig. 1, sorted by phase. Note towards the right the strong neutral iron lines (at 5167.487 and 5171.595 Å) and the strong neutral magnesium triplet (at 5167.33, 5172.68, and 5183.61 Å).

Radial velocities were determined using the Rucinski broadening functions (Rucinski 2004, Nelson 2010b, Nelson et al. 2014). An Excel worksheet with built-in macros (written by him) was used to do the necessary RV conversions to geocentric and back to heliocentric values (Nelson 2010a). The resulting RV determinations are also presented in Table 1. These results were corrected 5.2% up for the 2015 data, but only 1% for the 2016 data (owing to the shorter exposure times) to allow for the small phase smearing. Correction was achieved by dividing the RVs by the factor $f = (\sin X)/X$; where $X = 2\pi t/P$, where t denotes exposure time and P denotes the orbital period. For spherical stars, this

Table 1: Log of DAO observations.

DAO Image No.	Mid Time (HJD–2400000, d)	Exposure (sec)	Phase at mid-exp	RV_1 (km/s)	RV_2 (km/s)
13277	57299.7801	2400	0.839	+189.4(6.2)	−123.5(7.9)
13286	57299.8831	2400	0.169	−269.2(5.6)	+72.6(7.9)
13321	57300.6639	2400	0.678	+207.5(7.9)	−150.8(7.8)
13335	57300.8815	2400	0.377	−193.9(3.7)	+56.4(4.5)
9359	57646.7883	1200	0.719	+219.5(8.6)	−141.3(7.0)
9489	57652.8783	900	0.285	−267.4(6.5)	+76.9(9.7)

correction is exact; in other cases, it can be shown to be close enough for any deviation to fall below observational errors. The mean rms errors for RV_1 and RV_2 are 6.4 and 7.5 km/s, respectively, and the overall rms deviation from the (sinusoidal) curves of best fit is 9.7 km/s. The best fit yielded the values $K_1 = 256.6(1.1)$ km/s, $K_2 = 118.1(1.1)$ km/s and $V_\gamma = -30.5(0.6)$ km/s, and thus a mass ratio $q_{\rm sp} = K_1/K_2 = M_2/M_1 = 2.17(2)$.

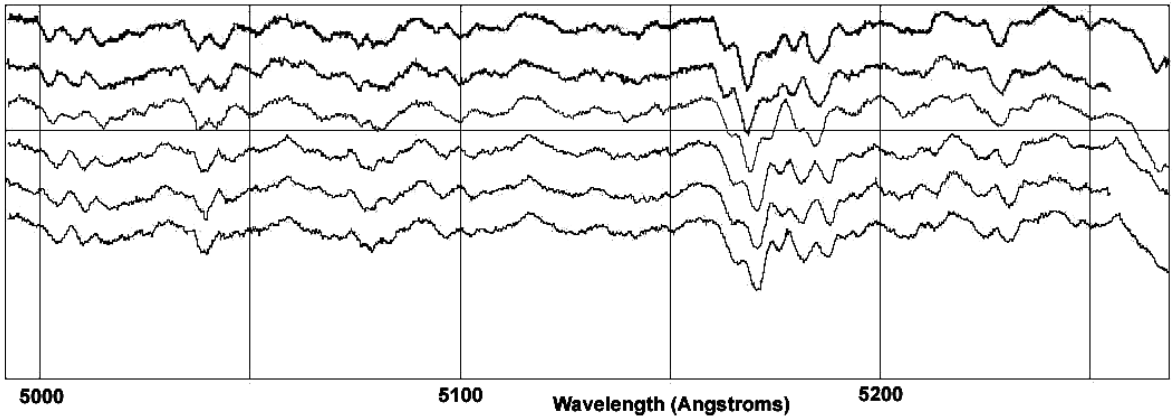

Figure 1. V2477 Cyg spectra at phases 0.169, 0.285, 0.377, 0.678, 0.719, 0.839 (from top to bottom).

Representative broadening functions, at phases 0.285 and 0.719 are depicted in Figs. 2 and 3, respectively. Smoothing by a Gaussian filter is routinely done in order to centroid the peak values for determining the RVs.

In May 8-11 of 2015, the author took a total of 201 frames in V, 204 in R_C and 199 in the I_C band at his private observatory in Prince George, BC, Canada. The telescope was a 33 cm f/4.5 Newtonian on a Paramount ME mount; the camera was a SBIG ST-10XME. Standard reductions were then applied. The variable, comparison and check stars are listed in Table 2. The coordinates and magnitudes for V2477 Cyg are from the Tycho Catalogue (Hog et al. 2000), those for the other two stars are from the GSC catalogue.

The author used the 2003 version of the Wilson-Devinney (WD) light curve and RV analysis program with Kurucz atmospheres (Wilson & Devinney 1971, Wilson 1990, Kallrath et al. 1998) as implemented in the Windows front-end software `WDwint` (Nelson 2009) to analyze the data. To get started, the spectral type F8 (taken from SIMBAD, no reference given; main sequence assumed) was adopted. Interpolated tables from Cox (2000) gave a temperature $T_1 = 6250 \pm 216$ K and $\log g = 4.367 \pm 0.006$. (The quoted er-

Table 2: Details of the variable, comparison and check stars.

Object	GSC	RA (J2000)	Dec (J2000)	V (mag)	$B-V$ (mag)
Variable	3945-1423	$20^{\rm h}18^{\rm m}58\overset{\rm s}{.}9357$	$56°36'19\overset{''}{.}272$	10.00(3)	+0.67(5)
Comparison	3495-1732	$20^{\rm h}19^{\rm m}33\overset{\rm s}{.}13$	$56°34'16\overset{''}{.}33$	10.44(5)	+1.063
Check	3945-1197	$20^{\rm h}18^{\rm m}52\overset{\rm s}{.}0$	$56°31'32\overset{''}{.}0$	10.7	N/A

rors refer to one and one half spectral sub-classes.) An interpolation program by Terrell (1994, available from Nelson 2009) gave the Van Hamme (1993) limb darkening values; and finally, a logarithmic (LD = 2) law for the limb darkening coefficients was selected, appropriate for temperatures < 8500 K (ibid.). The limb darkening coefficients are listed in Table 3. (The values for the second star are based on the later-determined temperature of 5880 K and assumed spectral type of G1.) Convective envelopes for both stars were used, appropriate for cooler stars (hence values gravity exponent $g = 0.32$ and albedo $A = 0.500$ were used for each).

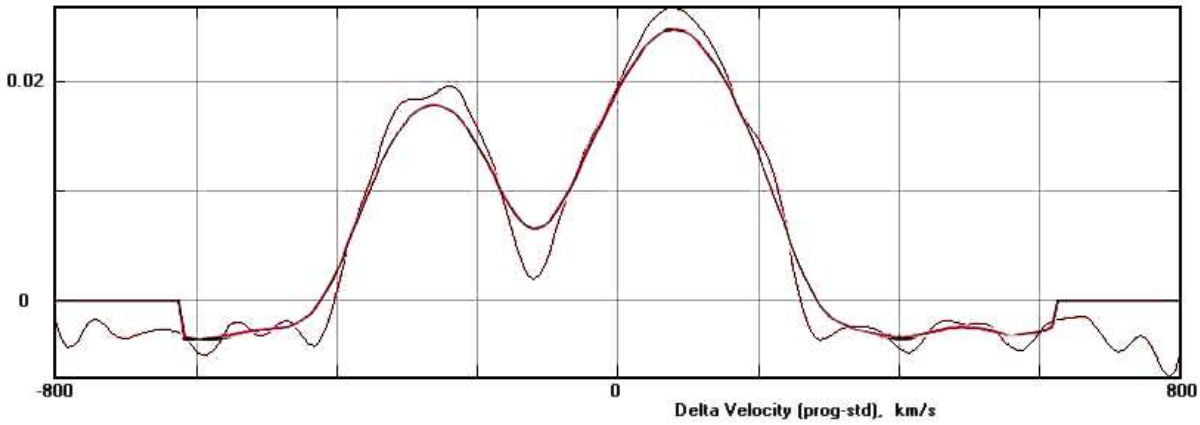

Figure 2. Broadening function at phase 0.285–smoothed and unsmoothed.

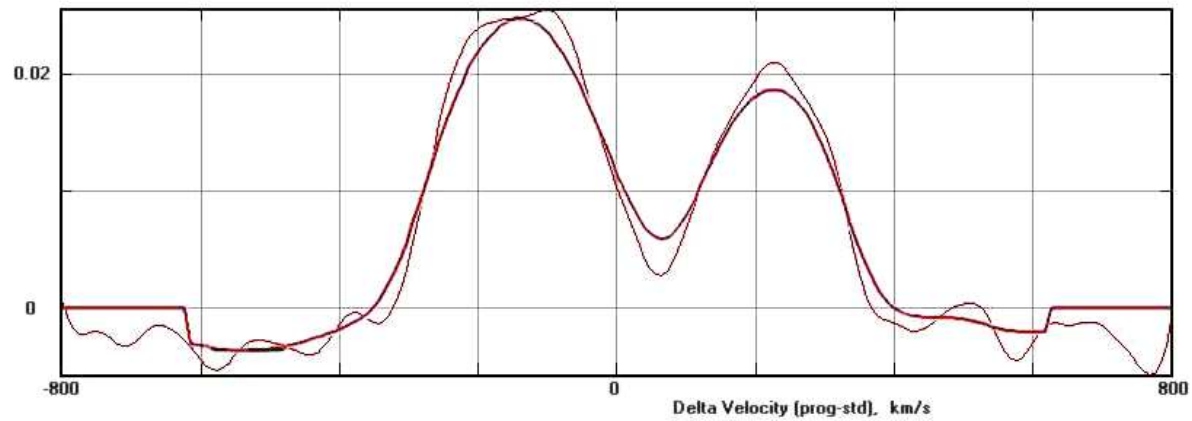

Figure 3. Broadening function at phase 0.719–smoothed and unsmoothed.

Table 3: Limb darkening values from Van Hamme (1993).

Band	x_1	x_2	y_1	y_2
Bol	0.647	0.647	0.179	0.214
V	0.790	0.755	0.164	0.242
R_C	0.723	0.684	0.203	0.260
I_C	0.637	0.600	0.212	0.254

From the GCVS 4 designation (EW) and from the shape of the light curve, mode 3 (contact binary) mode was used. Early on, it was noted that the maxima between eclipses were slightly unequal. This is the O'Connell effect (Davidge & Milone 1984, and references therein) and is usually explained by the presence of one or more star spots. Because of the only slight difference between Max I (phase 0.25) and Max II (phase 0.75), a solution was first sought with no spots; later on, one was added first to star 2, and then to star 1. The latter gave better results and was adopted. In any case, the spotted solution gave only a marginal improvement in the fit. However, both unspotted and spotted solutions are presented in Table 4, even though the values are identical in most cases.

Convergence by the method of multiple subsets was reached in a small number of iterations. (The subsets were: (a, i, Ω_1, L_1), (i, T_2, q), and (V_γ, i, Ω_1). Almost immediately, it was realized that a solution was impossible without third light (el_3). Therefore third light was added to the preliminary fitting, and that parameter was added to the third subset. Also, only values of the inclination near 90° were possible, with 90° always giving the best fit. In view of the fact that differential corrections always suggested non-physical corrections, the inclination was not varied thereafter.

Detailed reflections were tried, with $n_{\rm ref}$ = 1-3, but there was little—if any—difference in the fit from the simple treatment. There are certain uncertainties in the process (see Csizmadia et al. 2013, Kurucz 2000). On the other hand, the solution is very weakly dependent on the exact values used.

In the first set of iterations (i.e., with no spot), when a fit was near, the sigmas for each dataset were adjusted, based on the output of WD (viz. computed from the sum of residuals for each dataset plus number of points).

The model is presented in Table 4. For the most part, the error estimates are those provided by the WD routines and are known to be low; however, it is a common practice to quote these values and we do so now. Also, estimating the uncertainties in temperatures T_1 and T_2 is somewhat problematic. A common practice is to quote the temperature difference over—say—one and one half spectral sub-classes (assuming that the classification is good to one or two spectral sub-classes, the precision being unknown). In addition, various different calibrations have been made (Cox 2000, page 388–390 and references therein, and Flower 1996), and the variations between the various calibrations can be significant. If the classification is ± one sub-class, an uncertainty of ± 200 K to the absolute temperatures of each, would be reasonable. (The modelling error in temperature T_2, *relative to* T_1, is indicated by the WD output to be much smaller, around 5 K.)

The light curve data and the fitted curves are depicted in Figures 4-6. The residuals (in the sense observed-calculated) are also plotted, shifted upwards by 0.45 units.

The radial velocities are shown in Fig. 7. A three-dimensional representation from Binary Maker 3 (Bradstreet 1993) is shown in Fig. 8.

Table 4: Wilson-Devinney parameters.

WD	No spot	Spot		
Quantity	Value	Value	error	Unit
Temperature T_1	6250	6250	[fixed]	K
Temperature T_2	5879	5880	5	K
$q = m_2/m_1$	1.919	1.919	0.002	—
Potential $\Omega_1 = \Omega_2$	5.026	5.026	0.003	—
Inclination, i	90	90	[fixed]	deg
Semi-maj. axis, a	2.39	2.39	0.03	$R_\odot$
V_γ	−28.9	−30.1	2.7	km/s
Fill-out, f	0.1204	0.1204	—	—
Spot co-latitude	—	75	10	deg
Spot longitude	—	147	2	deg
Spot radius	—	18	2	deg
Spot temp. factor	—	0.976	0.002	—
el (V)	0.085	0.085	0.002	—
el (R_C)	0.084	0.084	0.002	—
el (I_C)	0.083	0.083	0.002	—
$L_1/(L_1 + L_2)$ (V)	0.4198	0.4196	0.0007	—
$L_1/(L_1 + L_2)$ (R_C)	0.4094	0.4093	0.0006	—
$L_1/(L_1 + L_2)$ (I_C)	0.4013	0.4012	0.0007	—
r_1 (pole)	0.3130	0.3130	0.0004	orb. rad.
r_1 (side)	0.3283	0.3283	0.0005	orb. rad.
r_1 (back)	0.3675	0.3675	0.0008	orb. rad.
r_2 (pole)	0.4204	0.4204	0.0003	orb. rad.
r_2 (side)	0.4483	0.4483	0.0004	orb. rad.
r_2 (back)	0.4805	0.4805	0.0006	orb. rad.
Phase shift	−0.0007	−0.0007	0.0001	—
$\Sigma\omega^2_{\rm res}$	0.06952	0.06335	—	—

The WD output fundamental parameters and errors are listed in Table 5. Corresponding values from the spotted and unspotted solutions agreed within the displayed digits in all cases, so therefore only one set of values is given. Most of the errors are output or derived estimates from the WD routines. From Kallrath & Milone (1998), the fill-out factor is $f = (\Omega_{\rm I} - \Omega)/(\Omega_{\rm I} - \Omega_{\rm O})$, where Ω is the modified Kopal potential of the system, $\Omega_{\rm I}$ is that of the inner Lagrangian surface, and $\Omega_{\rm O}$, that of the outer Lagrangian surface, was also calculated.

To determine the distance r, the analysis proceeded as follows: first the WD routine gave the absolute bolometric magnitudes of each component; these were then converted to the absolute visual (V) magnitudes of both, $M_{V,1}$ and $M_{V,2}$, using the bolometric corrections BC = –0.160 and –0.190 for stars 1 and 2 respectively. The latter were taken from interpolated tables constructed from Cox (2000). The absolute V magnitude was then computed in the usual way, getting $M_V = 4.14 \pm 0.03$ magnitudes. The apparent magnitude in the V passband was $V = 10.00 \pm 0.03$, taken from the Tycho values (Hog, et al., 2000) and converted to a Johnson magnitude using relations due to Henden (2001). The colour excess (in $B - V$) was obtained in the usual way, by subtracting the tabular value of $B - V$ (for that spectral class) from the observed (converted Tycho) value. This

gave E$[B-V] = 0.18$ magnitudes. However, reference to the dust tables of Schlegel et al. (1998) revealed a value of E$[B-V] = 0.2823$ for those galactic coordinates. Since the E$[B-V]$ values have been derived from full-sky far-infrared measurements, they therefore apply to objects outside of the Galaxy; this value of E$[B-V]$ so derived then represents an upper limit for closer objects within the Galaxy. Hence the lower value of 0.18 is reasonable, and was adopted. (An uncertainty of—say—half this amount was used in the error calculation for distance.)

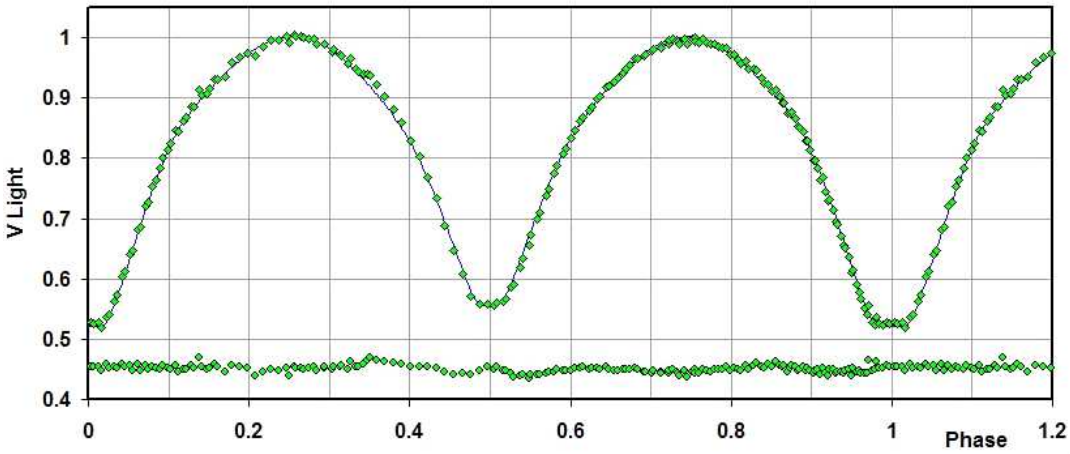

Figure 4. V light curves for V2477 Cyg – data, WD fit, and residuals.

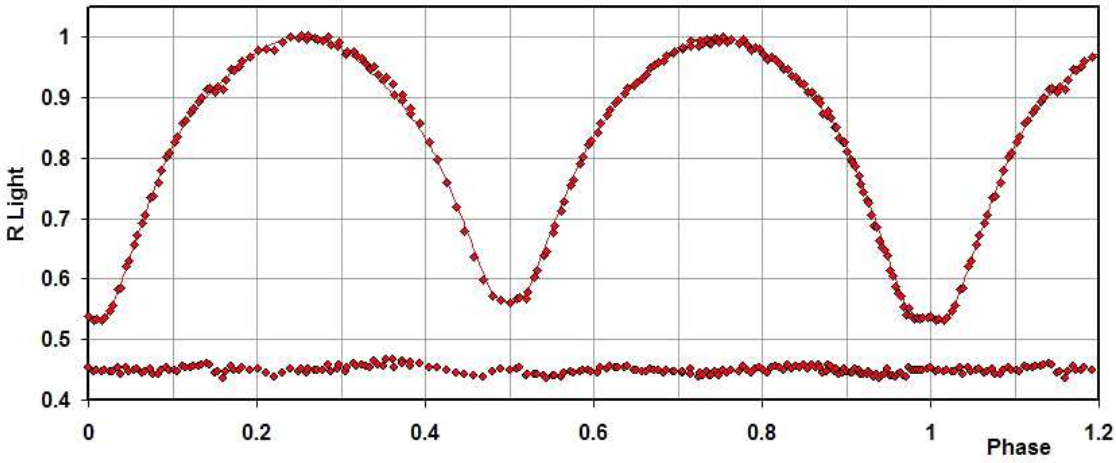

Figure 5. R_C light curves for V2477 Cyg – data, WD fit, and residuals.

Galactic extinction was obtained from the usual relation $A_V = R\mathrm{E}[B-V]$, using $R = 3.1$ for the reddening coefficient. Hence, distance $r = 112$ pc was calculated from the standard relation:

$$r = 10^{0.2(V-M_V-A_V+5)} \text{ pc} \qquad (2)$$

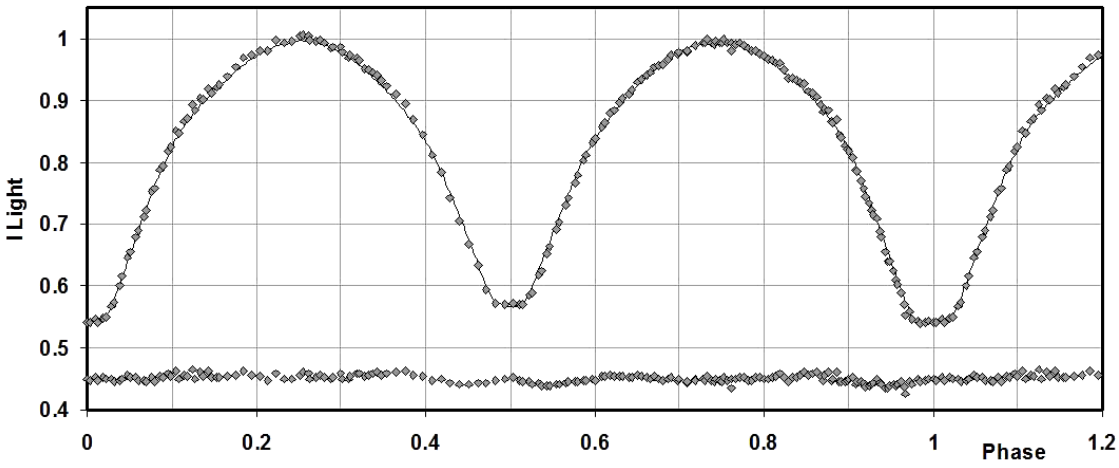

Figure 6. I_C light curves for V2477 Cyg – data, WD fit, and residuals.

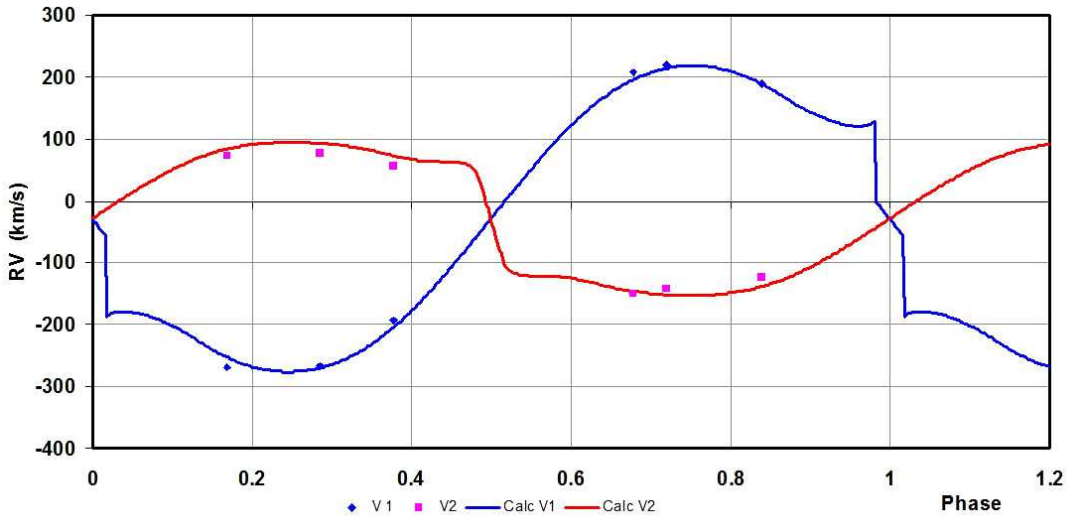

Figure 7. Radial velocity curves for V2477 Cyg – data and WD fit.

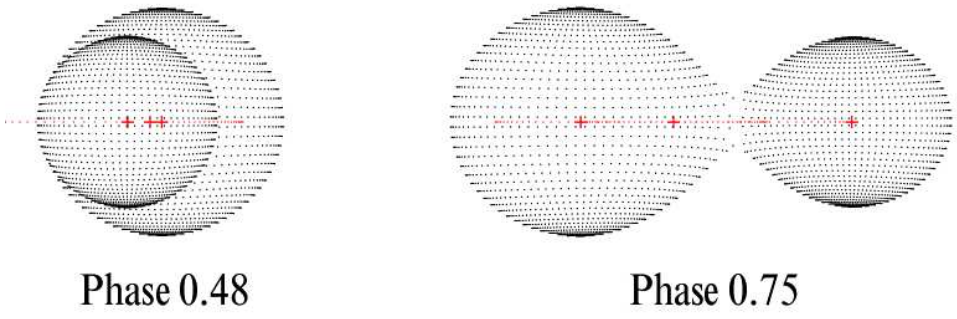

Figure 8. Binary Maker 3 representation of the system – at phases 0.48 and 0.75.

Table 5: Fundamental parameters.

Quantity	Value	Error	unit
Temperature, T_1	6250	200	K
Temperature, T_2	5880	200	K
Mass, m_1	0.65	0.02	$M_\odot$
Mass, m_2	1.24	0.02	$M_\odot$
Radius, R_1	0.81	0.01	$R_\odot$
Radius, R_2	1.08	0.01	$R_\odot$
$M_{\rm bol,1}$	4.91	0.02	mag
$M_{\rm bol,2}$	4.55	0.02	mag
log g_1	4.43	0.01	cgs
log g_2	4.47	0.01	cgs
Luminosity, L_1	0.895	0.02	$L_\odot$
Luminosity, L_2	1.25	0.02	$L_\odot$
Fill-out factor	0.12	0.005	—
Distance, r	112	15	pc

The errors were assigned as follows: $\delta M_{\rm bol,1} = \delta M_{\rm bol,2} = 0.014$, $\delta BC_1 = \delta BC_2 = 0.015$ (the variation of 1.5 spectral sub-classes), $\delta V = 0.03$, $\delta E(B–V) = 0.07$, all in magnitudes, and $\delta R = 0.1$. Combining the errors rigorously (i.e., by adding the variances) yielded an estimated error in r of 15 pc.

Some comments regarding the period variation are in order. An eclipse timing difference $(O - C)$ plot is depicted in Fig. 9. It will be seen that even though the existing points, almost all derived using CCD detectors, display considerable scatter, it is still possible to fit a quadratic relation. (Notes: for determining the elements of equation 1, a tangent line was used, and the open square represents a rejected datum.) But what should one do with the original point from 1999 (at cycle 0)?

Rucinski et al. (2007 and references therein) showed that, for close binaries, a third component is very common. So therefore the light time effect (LiTE) (whereby the orbiting pair makes an orbit about the common centre of mass, and the light information may be advanced or retarded due to varying distance to the observer), may play a role in the period variation. Irwin (1952, 1959) provided the equations for computing the theoretical period variation, based on the period of the third star, P_3 and other orbital parameters.

Using these equations, it is possible to fit not one but many (at least seven) different LiTE relations to all the points using periods P3 ranging from 14 to 35 years. It is obvious that no definitive solution for the orbital parameters of the putative third star orbit will be possible without many new points spanning perhaps a decade or more. However the point is that it is at least plausible that the light time effect exists and that the point at 0,0 is not aberrant. The $O - C$ file may be found online at Nelson (2016).

In conclusion, the fundamental parameters of this system have been determined. It has been shown to have a low degree of contact, expressed by the fill-out parameter $f = 0.120$. This is typical for a W-type contact binary (Rucinski 1974). Also, the existence a significant third light is consistent with the high proportion of contact binaries having a third component (Rucinski 2007, and references therein).

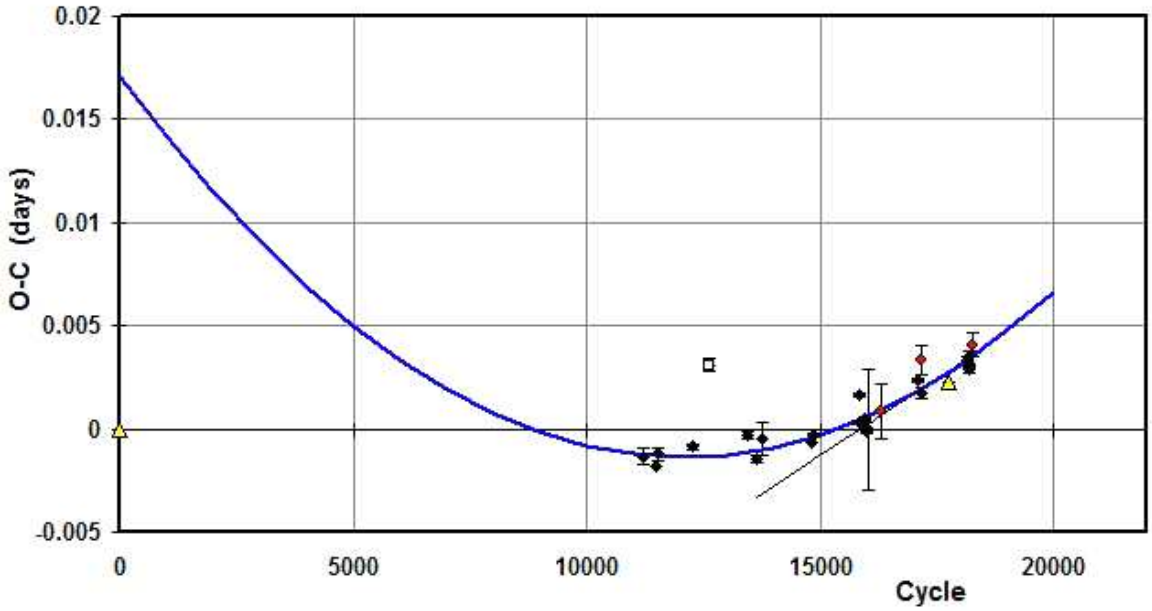

Figure 9. V2477 Cyg – eclipse timing $(O-C)$ diagram with a quadratic fit for points after cycle 10000.

No evidence of the third star was seen in the spectra. This is hardly surprising because of the relatively weak contribution from the third light. Because the relative flux at phases 0.25 and 0.75 has been normalized to close to unity, quantity l_3 represents the fractional contribution to the flux there (Wilson 1998, page 5). Assuming isotropic radiation from the third star, then its luminosity may be estimated by $\mathrm{el}_3 \times$(total luminosity of system) $= 0.04 \times 2.1 = 0.08$. If the companion is a main sequence star, this would make it a red dwarf of spectral type M1–M2—far too faint to register in the spectra above the noise.

It is somewhat troubling that the spectroscopic mass ratio $q_{\mathrm{sp}} = 2.17(2)$ differs significantly from that derived by the light curve modelling, $q_{\mathrm{ptm}} = 1.919(2)$. In view of the fact that the eclipses are total, we may trust the photometric value (Terrell & Wilson 2005). Moreover, the excellent fit of theoretical to observed light curves (Figs. 4-6) gives one confidence in the photometric value. But why is the spectroscopic value deviant?

It is tempting to believe that more spectra would clarify the situation, but there is much to be said for these spectra: they have a high signal-to-noise ratio, with continuum levels ranging from 20,000 to over 50,000; unlike some cases, the spectra reproduced in Fig. 1 display highly significant shifts over phase; the broadening functions, as reproduced in Figs. 2 and 3, are robust, with low noise and little to compromise the RV extraction; and finally, all estimates for the RV errors lie somewhat less than 10 km/s, typical in this work.

Although it has been argued that the contribution from the third star is low, it seems possible that its light has contaminated the spectra, distorting the RV determination.

Whatever the cause of the disparity, it seems safe to assume that the photometric mass ratio is more reliable and that the derived fundamental parameters are reliable.

Acknowledgements: It is a pleasure to thank the staff members at the DAO (especially Dmitry Monin and David Bohlender) for their usual splendid help and assistance.

References:

Bradstreet, D.H., 1993, "Binary Maker 2.0 - An Interactive Graphical Tool for Preliminary Light Curve Analysis", in Milone, E.F. (ed.) Light Curve Modelling of Eclipsing Binary Stars, pp 151-166 (Springer, New York, N.Y.)
Cox, A.N., ed, 2000, Allen's Astrophysical Quantities, 4th ed., (Springer, New York, NY)
Csizmadia, S., Pasternacki, T., Dreyer, C., Cabrera, A., Erikson, A., Rauer, H., 2013, *A&A*, **549**, A9 DOI
Davidge, T.J., Milone, E.F., 1984, *ApJS*, **55**, 571 DOI
Flower, P.J., 1996, *ApJ*, **469**, 355 DOI
Gessner, H., 1966, *Veröff. Sternwarte Sonneberg*, **7**, 61
Henden, A., 2001, `http://www.tass-survey.org/tass/catalogs/tycho.old.html`
Hoffmeister, C. von, 1963, *AN*, **287**, 169 DOI
Hog, E., et al., 2000, *A&A*, **355**, L27
Irwin, J.B., 1952, *ApJ*, **116**, 211 DOI
Irwin, J.B., 1959, *AJ*, **64**, 149 DOI
Kallrath, J., Milone, E.F., 1998, Eclipsing Binary Stars–Modeling and Analysis (Springer-Verlag) DOI
Kallrath, J., Milone, E.F., Terrell, D., Young, A.T., 1998, *ApJ*, **508**, 308 DOI
Kurucz, R.L., 2000, *Baltic Astron.*, **11**, 101
Nelson, R.H., 2009, software by Bob Nelson, `http://members.shaw.ca/bob.nelson/software1.htm`
Nelson, R.H., 2010a, spreadsheets by Bob Nelson, `http://members.shaw.ca/bob.nelson/spreadsheets1.htm`
Nelson, R.H., 2010b, "Spectroscopy for Eclipsing Binary Analysis" in The Alt-Az Initiative, Telescope Mirror & Instrument Developments (Collins Foundation Press, Santa Margarita, CA), R.M. Genet, J.M. Johnson and V. Wallen (eds)
Nelson, R.H., 2016, Bob Nelson's $O-C$ Files, `http://www.aavso.org/bob-nelsons-o-c-files`
Nelson, R. H., Şenavcı, H.V. Baştürk, Ö., Bahar, E., 2014, *New Astron.*, **29**, 57 DOI
Otero, S.A., Wils, P., 2005, *IBVS*, **5630**
Rucinski, S. M., 1974, *AcA*, **24**, 119
Rucinski, S. M., 2004, *IAUS*, **215**, 17
Rucinski, S. M., Pribulla, T., and van Kerkwijk, M.H., 2007, *AJ*, **134**, 2353 DOI
Schlegel, D.J., Finkbeiner, D.P., Davis, M., 1998, *ApJ*, **500**, 525 DOI
Skiff, B.A., 1999, *IBVS*, **4720**
Terrell, D., 1994, Van Hamme Limb Darkening Tables, vers. 1.1.
Terrell, D. Wilson, R.E., 2005, *ApSS*, **296**, 221 DOI
Van Hamme, W., 1993, *AJ*, **106**, 2096 DOI
Wilson, R.E., Devinney, E.J., 1971, *ApJ*, **166**, 605 DOI
Wilson, R.E., 1990, *ApJ*, **356**, 613 DOI
Wilson, R.E., 1998, Documentation of Eclipsing Binary Computer Model (available from the author)